

Global Stiffness Structural Optimization for 3D Printing under Unknown Loads

Tuanfeng Y. Wang^{1,2}, Yuan Liu¹, Xuefeng Liu³, Dongming Yan⁴, Ligang Liu¹, Jiansong Deng¹, Falai Chen¹, Zhouwang Yang¹

¹ University of Science and Technology of China

² University College London

³ Niigata University

⁴ VCC, KAUST

Abstract

The importance of the stiffness of a 3D printed object has been realized gradually nowadays. Unlike industry product using *stiff-but-weak* materials such as metal, cement, etc. using stress as criterion is not suitable when considering the problem of 3D printing as materials used here (ABS, Nylon, resin, etc.) is rather elastic – which is the case of *flexible-but-strong*. 3D printed objects are always hollowed with interior structure to make the fabrication process cost-effective while maintain the stiffness. State-of-the-art techniques are either *redundant design* (using an amount of materials much more than necessary to ensure the stiffness in any case) or optimizing the structure under one of the most-possible loads distributions which fall short in other distribution cases. We propose a novel approach for designing the interior of the object by optimizing the global stiffness – minimizing the maximum deformation under any possible load distribution. We first simulate the object by a lightweight frame structure and optimize both the size and the geometry using an eigen-mode-like formulation, interleaving with a topology clean. A postprocess is applied to generate the final object based on the optimized frame structure. Optimizing the interior structure under unknown loads automatically keeps reinforce where the structure is the weakest and is proved to be a powerful and more reasonable design framework in our experimental results.

1 Introduction

The 3D printing technique provides a powerful solution to prototype customized objects with fine surface details and complex interior structures. However, the spread and development of this technique is hindered to the high cost of material and low speed of fabrication. Research efforts have been devoted to reduce the material used, i.e., the volume/weight of object, and the key challenge here is to keep the stiffness while less material is used. Given a load distribution, it is natural to hollow the object for a cost-effective purpose and add interior structure to optimize the structure stiffness-to-weight ratio [11, 19, 24]. Such load-distribution-based techniques have been highly successful in ideal cases as perfectly minimizing the structural deformation/stress with much less material in real world physical test with corresponding preset loads. However, they are not suitable for many real world applications because the loads on a fabricated object may appear in other distributions which are different from the preset one. As shown in Figure 1(a), the Trophy model could be held in many different ways which lead to very different load distribution cases.

Instead of taking one (or several) load distribution case(s) into consideration, we optimize the global stiffness-to-weight ratio by minimizing the maximum of deformation under any load distribution cases, named as unknown loads due to no load distribution case is given to be based on. We use the criterion *deformation* rather than *stress*, as the former is more suitable when using elastic materials like many materials in 3D printing. Such elastic property preserve the fabricated object from breaking under large stress but is much easier to be deformed when load is applied. The rationality of the deformation based formulation can coincidently be supported by previous research as well (see details in Sec. 3.3). When the amount of material is given, our unknown-load-based optimization framework aims to make the object perform the best (stiffest) among other interior design when the corresponding worst (lead to the largest deformation) load distribution case is applied.

Our work is inspired by the research of [5] and [24]. These work show that an entire object can be simulated by a frame structure consisting of a set of beams and a set of nodes connected by these beams. Frame structure captures most of the structural features of the object and has a rather small set of parameters which can be analyzed and computed with high efficiency. The last step of our framework restores the optimized frame structure back to an entity object ready to be fabricated and the global stiffness property is proved to be kept.

Prior to global stiffness optimization, we first perform a *Constrained Centroidal Voronoi Tessellation* (CCVT) on the input object and obtain an isotropic initial frame by taking the edges of each tetrahedron as beam of the initial frame. The global stiffness problem is then formulated as a saddle point problem by minimizing the maximum norm of the deformation under any normalized load. Optimization on nodes positions, beam radii and nodes topology connections are applied to the frame structure using a saddle point algorithm. After optimization algorithm is terminated, we adopt a postprocess step to generate the object with original object surface and lightweight interior based on the optimized frame structure. Note that it is not simply cover a skin on the frame structure like [24]. As the skin can not be analyzed efficiently, our postprocess is rather like an adaptive hollowing meanwhile adding interior supportive structure. Finally, we use the *Finite Element Method* (FEM) to analyze and verify the rationality of our results.

2 Related Work

Significant efforts have been made recently on fabrication-aware 3D shape design which establishes physically-fabricated prototypes and manufactured objects using 3D printing. Previous work focused on the desire of certain physical properties, such as deformation behavior [3], fabricatable via commercial 3D printer's limited working volume [12], physical realization [19], stability

Email: Tuanfeng.wang@cs.ucl.ac.uk

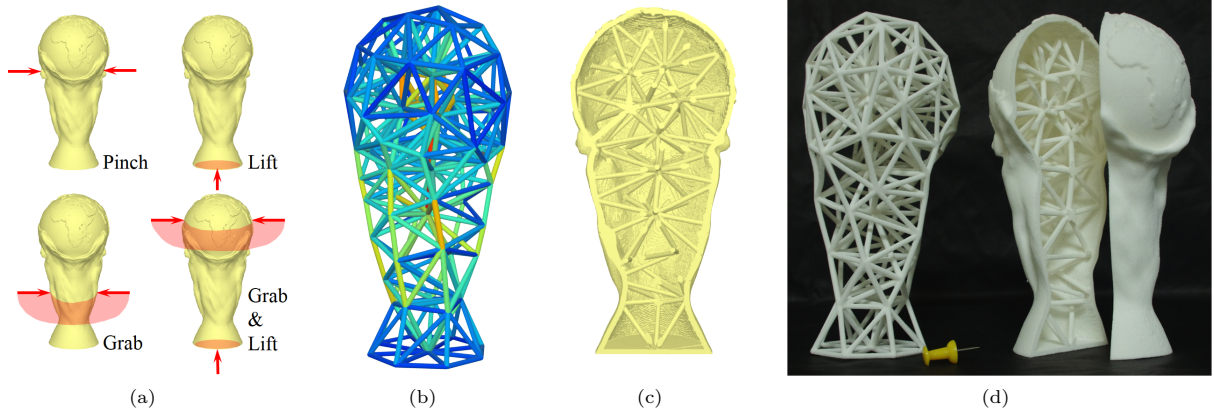


Figure 1: For the Trophy model (a), a user could hold it in many possible gestures but this remains uncertain during the interior design for a cost-effective purpose. With a given amount of material, our algorithm first produces a global stiffness frame structure (b) under unknown loads, by minimizing the maximal deformation (colored according to beam radii). (c) is the sectional view of the object generated from the optimized frame structure, and (d) is the photo of the printed frame and the object generated by our method. A yellow standard pin is placed next to the object as the size reference.

over gravity on certain orientation [1, 15]. These work fully developed the benefit of 3D printing over traditional CNC fabrication techniques because both fine surface details and complex interior structure are able to be fabricated.

Over the recent years it has been more and more recognized that 3D printing techniques, including FDM/SLS/SLA, etc., are hindered for both research and commercial purposes by such a high material cost and a rather low fabrication speed. The core problem here is to reduce the designed volume of the object. Inspired by lightweight structure observed from nature, [11, 24] adopted lightweight structures to fill the object rather than solid interior. These work optimize the stiffness/strength-to-weight ratio under a given external force while the original object surface is preserved. However, the results of these load-based methods fall short in real world cases as load distribution applied by user is always different from the ideal preset case. With a novel formulation, our proposed unknown-load-based method perfectly solves this problem by optimizing and generating a global stiffness design with a uniform framework. Without a given load distribution, [21] presents a structural analysis technique that slice the object into cross-sections and compute stress based on bending momentum equilibrium. For a similiar purpose, a finite element based structural analysis method is presented in [27]. Based on experimental observation, this work uses an Eigenmode formulation to detect the weakest area of an object. In our paper, this observation is proved mathematically from our global stiffness formulation. In computational structure area, structure analysis and optimization under unknown load distribution have been discussed during the past few years, such as [6, 7, 20]. These work, although sharing the same target, test different kinds of object functions without a proof of rationality. These work also limited the problem into 2D domain and focus on only geometry rather than take all variables (size, geometry, topology) into consideration, which is far from a complete solution of the cost-effective fabrication challenge.

In order to reduce the volume of the object, lightweight structure is adapted for supportive interior. The design and optimization of lightweight structures have been extensively explored in tissue engineering and computer-aided design. Smith et al. [18] focus on optimizing the design of truss structures where beams connected by pin joints are rotation-free and difficult to preserve the geometrical shape of the object. Using lightweight structures for improving the strength and the stiffness of objects has also been studied in the field of rapid manufacturing [23], where the particle swarm optimization or generic algorithms were selected to search for design solutions. Detailed reviews on various aspects of structural optimization can be found in [2]. Due to the differences in the types of objectives and constraints, the approaches there are not suitable for our purpose of 3D printing.

We use the frame structure in the lightweight design for its fabrication-friendly. Each beam in the frame structure is considered as the basic element which is different from classical structural topology optimization methods. Structural topology optimization is employed mainly to specify the optimum number and location of holes in the configuration of the designed structure. Element-based methods for structural topology optimization decompose the volume of the input object into finite-element-like tetrahedrons, or a grid-like structure for analysis. The *Optimality Criteria* (OC) [16] methods are proved to be among the most effective element-based methods for solving topology optimization problems. A recent review of this area is offered by [17]. It is easy to extend our framework into element-based computation, however, due to the linear elastic property of frame structure, taking a single beam as basic element is much more efficient.

3 Problem and formulation

Problem. The input of our framework is the surface mesh S . Our goal is to generate an entity global stiffness object model H consisting of an adaptive hollowed shell and a supportive interior structure, while utilizing no more than a given amount of material. The generated object shares the same surface with S but has much less weight than S for its lightweight supportive structure rather than solid filled.

Remarks The following two problems are usually considered in the structural optimization: Stiffness-to-Weight and Weight-to-Stiffness. Stiffness-to-Weight is to design a structure with the maximum stiffness using a specific amount of given material; and Weight-to-Stiffness is to design a structure with the least amount of material but satisfied the given stiffness expectation. These two problems are dual and can be converted to each other by a simple binary search process. Without loss of generality, here we focus on the former one that takes the amount of material use as the constraint. We also consider the load is only from external forces as the internal forces, gravity for most of the time, remains very small compared with external forces so is ignored.

3.1 Frame structure

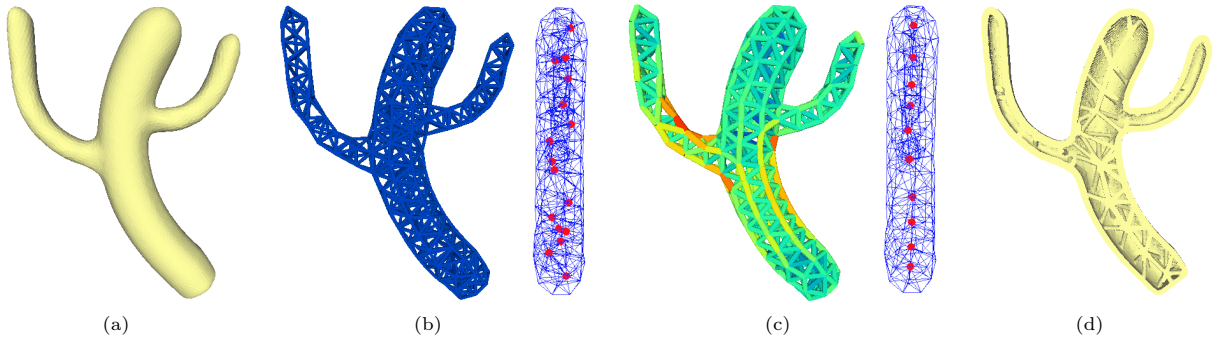
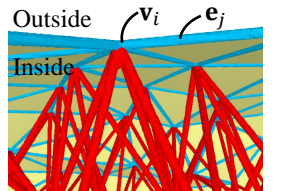


Figure 2: Pipeline of our approach. Given an input model (a), an initial frame structure (b) is generated. Our method runs a saddle point algorithm to obtain an optimized frame structure (c) which provides minimal deformation under unknown load distribution. (c) is colored to visualize their radii and a side view of the frame structure is presented to show the node position and topology connections before and after optimization. Then a post-processing step is applied to generate a solid structure (d) for 3D printing. The front part of (d) is removed in order to show the internal structure.

A frame structure \mathcal{T} consists of a set of frame nodes $V = \{\mathbf{v}_i, i = 1, 2, \dots, m\}$ which are sampled on S (marked in yellow) and in the volume enclosed by S , as well as a set of frame beams $E = \{\mathbf{e}_j, j = 1, 2, \dots, n\}$ which are the edges connecting the nodes, as shown in the right figure. Each node \mathbf{v}_i represents a geometric position and each beam \mathbf{e}_j is a cylindrical shape with radius r_j and length l_j . Here \mathcal{T} can be seen as a graph of V and E with the geometry defining node positions, the beam radii, and the topology defining the connectivity between nodes. For convenience, we also denote $V_S = \{\mathbf{v}_i \mid \mathbf{v}_i \in S\}$, $V_I = V \setminus V_S$, $E_S = \{\mathbf{e}_j \mid \mathbf{e}_j \in S\}$ (marked in cyan), and $E_I = E \setminus E_S$ (marked in red).



By taking adequate density of surface points, the appearance of frame \mathcal{T} is expected to approximate S within a certain geometric error [25]. After the frame is optimized, surface edges of frame (i.e., E_S) indicate the adaptive thickness (doubled radius) of the surface shell around the position of the edges. Interior edges of the frame (i.e., E_I) are taken as cylinder-like supportive beams. And then the frame \mathcal{T} can be considered as a reasonable approximation of the final entity object \mathcal{H} .

The approach presented in this paper uses node positions and beam radii as design variables in the global stiffness structural optimization. This is different from element-based methods for structural topology optimization [17], where problems are expressed by tetrahedron-element-wise step functions. As an effective discrete representation, the frame structure is fabrication-friendly and has simple mechanical properties which will be described in Section 3.2.

3.2 Stiffness matrix

The mechanics of frame structure has been studied based on beam theory [4, 8, 9] where frame beams are assumed to behave like simple beams under linear deformation caused by nodes' displacement or rotation. In our method, we make the following assumptions in calculating the equilibrium state of the structure.

- a) The beams are only connected to each other at nodes.
- b) The beams are connected rigidly to have tensile, torsion, transverse shear force.
- c) Each node has three displacement degrees of freedom and three rotation degrees of freedom.

Linear relationship between deformation and force For a given frame structure, including both the surface and interior beams, the relationship between deformation —the displacement and rotation of each node, and the force (including torque) should satisfy the following discretized equilibrium equation.

$$K(V, \mathbf{r})D = F, \quad (1)$$

where $V = (\mathbf{v}_1, \dots, \mathbf{v}_m)$ also denotes the geometric positions of the nodes. $K(V, \mathbf{r})$ is the stiffness matrix, which depends on node positions V and beam radii $\mathbf{r} = (r_1, \dots, r_n)$. $F = (F_1, \dots, F_m)^T$ is the force and torque distribution acting on each node and $D = (d_1, \dots, d_m)^T$ is the displacement and the rotation of deformation caused by F . For details, refer to [4]. Note that F in Eq. (1) is the sum of external force and only acts on a special set of nodes like V_S . This is for a better simulation of real world cases because external forces are always act on the surface.

3.3 Eigen-Mode-like formulation

Our global stiffness target, which minimizes the maximum deformation under unknown loads can be described as an Eigen-Mode-like formulation.

Originally, for the frame structure simulated from an object, we first find an external force F that gives the maximal deformation. In order to avoid the scale problem, it is estimated by a deformation ratio $\frac{D^T D}{F^T F}$. Then we minimize the maximal deformation ratio of the frame structure by varying the design variables (V_I, \mathbf{r}).

For an object in the state of equilibrium, the following conditions for F are needed:

$$\mathbf{1} \cdot F_i = 0, \quad F_i \cdot (X_{i+1} - X_{c,i+1}) - F_{i+1} \cdot (X_i - X_{c,i}) = 0 \quad (2)$$

where $i = 1, 2, 3$; F_1, F_2, F_3 are force components of F along x , y , z axis respectively; X_1, X_2, X_3 are the lists of x -, y -, z -coordinates of the nodes X in a frame structure; $X_c = (X_{c,1}, X_{c,2}, X_{c,3})$ is the center point of the object. These two constraints indicate that both the force and the moment of the force are zero. Since stiffness matrix K is singular, for each F satisfying Eq. (2), to uniquely determine a solution $KD = F$, the translation and rotation should be ignored. Similar to Eq. (2), the total displacement and the total moment of displacement, the total rotation and the total moment of rotation are set to zero. Let the stiffness matrix under the above conditions on force and deformation be \hat{K} , which is now a regular matrix, then we have $D = \hat{K}^{-1}F$.

Thus, the structural optimization problem can be constructed as follows

$$\min_{(V_I, \mathbf{r}) \in \Theta} \max_{F \text{ satisfying (2)}} \frac{(\hat{K}^{-1} F)^T (\hat{K}^{-1} F)}{F^T F} \quad (3)$$

where Θ is the collection of all feasible V_I and \mathbf{r} ; see detailed constraints in Sec. 3.4.

Eigen-Mode property We here to discuss a more general situation if the external force can also act on V_I . As the stiffness matrix \hat{K} is symmetric, the vector F that maximizes the value $(\hat{K}^{-1} F)^T (\hat{K}^{-1} F)/F^T F$, according to [14], is just the eigenvector corresponding to the smallest eigenvalue of \hat{K} , denoted by $\lambda_{\min}(\hat{K})$ which is actually the same to the minimal positive eigenvalue of K . Finally, we have such an eigen-mode optimization problem

$$\max_{(V_I, \mathbf{r}) \in \Theta} \lambda_{\min}^*(K(V, \mathbf{r})) \quad (4)$$

where $\lambda_{\min}^*(K(V, \mathbf{r}))$ is the minimal positive eigenvalue of stiffness matrix $K(V, \mathbf{r})$.

In this way, our formulation mathmatically proof the observation given by [27] that the eigenvector of kinematic equation indicates a structural worst-case. Here our linear relationship between deformation and force (ignored the first derivative of force) is a static but more realistic version of the kinematic equation. Our global stiffness optimization, therefore, can also be considered as automatically reinforce where the structure is the weakest. On the other hand, plenty of physical experiments done by [27] can also show that our deformation based formulation is reasonable in calculating 3D Printed object.

3.4 Constraints on structure design parameters

Radius bounds To make the frame structure printable, the radius of each beam should be no less than the minimum printable radius \underline{r} . To avoid unrealistic design, an upper bound \bar{r} for the radius is imposed for each beam. Moreover, in order to retain the linear elastic property of the frame structure, the ratio between the length and the radius of a beam must satisfy the Euler buckling constraint. In brief, the buckling and the printability can be integrated as a bounded constraint for each beam radius

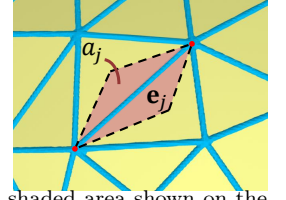
$$\underline{\eta}_j \leq r_j \leq \bar{r}, \quad \mathbf{e}_j \in E, \quad (5)$$

where $\underline{\eta}_j = \max(l_j/\alpha, \underline{r})$, l_j is the length of beam \mathbf{e}_j , and α is the slenderness ratio.

Volume The proposed problem is defined as optimizing the frame structure when a certain amount of material is given.

Let $\overline{\text{Vol}}$ be the amount of material available. The volume of solid material in the designed structure \mathcal{H} consists of two parts: the volume of interior beams in the frame, and the volume of adaptive-hollowed shell, which can be approximately calculated as the sum of the product of the area covered by a surface beam and its doubled radius. Thus we have a constraint on the material volume

$$\sum_{\mathbf{e}_j \in E_I} \pi r_j^2 l_j + \sum_{\mathbf{e}_j \in E_S} 2r_j a_j \leq \overline{\text{Vol}}, \quad (6)$$



where a_j is the area covered by beam \mathbf{e}_j on the surface. In practice, a_j is roughly calculated as the shaded area shown on the right.

Shape barrier The appearance of our optimal result should be the same with the surface of the input mesh. As a result, elements in internal beams set E_I have to be kept inside of the volume enclosed by S . Many algorithms have been developed for this purpose. In our implementation, an efficient but approximate method is adapted that several test points are sampled from each beam for a quick check whether they are inside S . A feasable solution of the optimization problem is subject to the constraint that all the test points are inside S .

Other constrains The objective function of our optimization is very flexible and can be solved efficiently. As a result, addition constrains are able to be considered in our formulation such as stability, self-supportiveness, orientation, angle of beams, etc., including printability constrains specified by certain printing techniques. In this paper, we focus on the main problem – global stiffness formulation, as these constrains have been well studied by many previous work [24].

4 Methodology

We propose a novel approach based on the formulation Eq. (3) to find a global stiffness structure which provides the best load-bearing performance under any possible load distributions. An overview of our algorithm is shown in Figure 2. Given a closed 3D input surface S represented by a triangular mesh, we first compute an isotropic initial frame with its beams of lower bound radii. We use the *Constrained Centroidal Voronoi Tessellation* (CCVT) [26] for this step (see Figure 2(b) for an example). Starting from this initial frame, we then iteratively optimize the beam radii and node position by solving a saddle point problem (see Figure 2(c)), to achieve a frame with maximum global stiffness under the volume constraint. Finally, we apply a post-processing step to the optimized frame structure to generate an entity object that inherits the global stiffness property as the final result (see Figure 2(d)).

4.1 Frame initialization

We choose an isotropic tetrahedralization approach [26] to guide the frame initialization, with a uniform density function, for our purpose. We first randomly generate a set of sites in the interior domain of surface S . The number of sites is specified by the user, it is related to the complexity of frame structure. Then we minimize the CCVT energy function by iteratively optimizing the positions of the sites. Once the optimization is terminated, the dual triangulation is extracted as the initial frame. This initial frame will be determined by having each tetrahedral edge as a frame beam with the radius $\underline{\eta}$ (defined in Eq. (5)). Although an adaptive initialization is considered to benefit the start point of optimization, it is actually ill-posed as our target is to strengthen the weakest. If the initialization is adaptive to the initial weakest situation, it will no longer benefit the final result as the weakest situaiton is changing during the optimization (see Fig. 4). On the other hand, an isotropic initialization is good enough as our geometry optimization is shown to contributed a lot to the final result (see Fig. 2(d)).

Remarks For thin details on the surface, damage can easily happen even without any hollowing. So as a part of the initialization, we first simplify all the thin parts and add these geometric details back only after the solid object is finally generated. This is automatically realized thanks to the natural limitation of CCVT, which eliminates thin parts by optimizing the energy function with a uniform density function.

4.2 Saddle point algorithm

In global stiffness structural optimization (3), derivatives of the objective function, e.g., gradients, with respect to V_I and \mathbf{r} cannot be explicitly expressed and efficiently calculated. It would be extremely unfavorable to employ most iterative strategies that make use of the first and probably second derivatives of the objective function. However, without using gradient information, the computational cost of using direct search methods would be too expensive and too time-consuming. Through rigorous mathematical derivation, we will present an algorithm based on the Rayleigh-quotient to greatly accelerate the solving of the problem.

We first define the Rayleigh-quotient [14] of the stiffness matrix $K(V, \mathbf{r})$ as

$$Q(V, \mathbf{r}, \mathbf{u}) = \frac{\langle K(V, \mathbf{r})\mathbf{u}, \mathbf{u} \rangle}{\langle \mathbf{u}, \mathbf{u} \rangle}. \quad (7)$$

According to the extremal property of Rayleigh quotient, the global stiffness structural optimization (3) is equivalent to the following saddle point problem

$$\max_{(V_I, \mathbf{r}) \in \Theta} \min_{\mathbf{u} \in N(K)^\perp} Q(V, \mathbf{r}, \mathbf{u}) \quad (8)$$

where $N(K)^\perp = \{\mathbf{u} \mid \mathbf{z}_i^T \mathbf{u} = 0, i = 1, \dots, 6\}$ is the orthogonal complement of $\text{Null}(K) = \text{span}\{\mathbf{z}_1, \dots, \mathbf{z}_6\}$. In the saddle point problem (8), the gradients $\{\nabla_V Q, \nabla_{\mathbf{r}} Q, \nabla_{\mathbf{u}} Q\}$ have explicit expressions and can be computed efficiently. Thus, we can design a Rayleigh-quotient based algorithm for optimizing the frame structure as follows.

Algorithm 1 Rayleigh-quotient based algorithm

Input: an initial frame $\mathcal{T}^{(0)}$ obtained in Section 4.1

Output: an optimized frame \mathcal{T} with its design variables (V_I, \mathbf{r})

Step 1: Get $(V^{(0)}, \mathbf{r}^{(0)})$ from the initial frame, obtain the eigenvector $\tilde{\mathbf{u}}^{(0)}$ corresponding to the minimal positive eigenvalue of $K(V^{(0)}, \mathbf{r}^{(0)})$, specify a threshold ϵ , and let $k := 1$.

Step 2: Update $(V_I^{(k)}, \mathbf{r}^{(k)}) = \arg \max_{(V_I, \mathbf{r}) \in \Theta} Q(V, \mathbf{r}, \tilde{\mathbf{u}}^{(k-1)})$ by the interior-point algorithm [13, Chapter 19].

Step 3: Compute the minimal positive eigenvalue of $K(V^{(k)}, \mathbf{r}^{(k)})$ and its corresponding eigenvector $\tilde{\mathbf{u}}^{(k)}$.

Step 4: If $Q(V^{(k)}, \mathbf{r}^{(k)}, \tilde{\mathbf{u}}^{(k)}) - Q(V^{(k-1)}, \mathbf{r}^{(k-1)}, \tilde{\mathbf{u}}^{(k-1)}) \leq \epsilon$, then output $(V^{(k)}, \mathbf{r}^{(k)})$ as optimized design variables for the final frame; Otherwise, go back to **Step 2**.

When the optimized frame is generated from our Rayleigh-quotient based algorithm, we will then merge any pairs of nodes that are connected by a strut that is at the minimum allowable length. The struts with small radii can also be eliminated to simplify the structure by applying a sparse optimization described in [24]. After this topology-cleaning step, we will use the optimized frame to generate a solid structure H for 3D printing.

4.3 Postprocess

The ultimate goal of our approach is to generate an entity object H inside the surface boundary S . For this purpose, we separate the optimized frame \mathcal{T} into the boundary beam set E_S and the interior beam set E_I , as discussed in Section 3.1. The beam sets E_S and E_I will guide the adaptive hollowing and interior structure generation, respectively.

First, the radii of the surface beams are used to determine a thickness function as

$$\zeta(\mathbf{p}) = 2(w_1 \cdot r_{j_1} + w_2 \cdot r_{j_2} + w_3 \cdot r_{j_3}), \quad \forall \mathbf{p} \in S,$$

where $\{r_{j_1}, r_{j_2}, r_{j_3}\}$ are the radii of three surface beams from triangle $\Delta \mathbf{e}_{j_1} \mathbf{e}_{j_2} \mathbf{e}_{j_3} \subset E_S$ where the point \mathbf{p} lies, and $\{w_1, w_2, w_3\}$ are its barycenter coordinates. Let $\Omega \subset \mathbb{R}^3$ be the region bounded by the input surface mesh S . Then the adaptive hollowed surface shell is defined as

$$H_S = \{\mathbf{q} \in \Omega \mid \|\mathbf{q} - \mathbf{p}\| \leq \zeta(\mathbf{p}), \forall \mathbf{p} \in S\}, \quad (9)$$

which can be considered as a piecewise linear interpolation of the surface beams E_S . Similarly, the beams in E_I are used to define the interior supportive structure as

$$H_I = \{\mathbf{q} \in \Omega \mid \text{dist}(\mathbf{q}, \mathbf{e}_j) \leq r_j, \forall \mathbf{e}_j \in E_I\}, \quad (10)$$

where $\text{dist}(\mathbf{q}, \mathbf{e}_j)$ is the geometric distance of point \mathbf{q} to the line segment \mathbf{e}_j . The whole solid structure H can then be given as

$$H = H_S \bigcup H_I.$$

Finally, we apply the *Extended Dual Contouring* (EDC) algorithm [22] to extract the 2-manifold surface boundary of solid H . As shown in Figure 2(d), the generated solid structure with its boundary mesh is now ready for 3D printing.

5 Results and discussion

In this section, we present some computational results of the proposed approach. Our approach offers a global stiffness design of interior structure with the input surface mesh and the amount of material allowed. Our algorithm is applied to a variety of objects that would be applied with different load distributions in regular use like American football, toys and models. We first verify the optimization results of our formulation with the analysis framework in Sec. 3.2, and then verify the final results of the whole framework which are generated based on the optimized frame structures. Different from verifying the result of optimization under given load, our global stiffness optimization result is difficult to test in real physical experiment but thanks to the advance of FEM technique, we examined our results based on a FEM-based computational framework that can be considered as a good simulation of physical experiment, which will be discussed later.

Criteria With a $10N$ load is applied, two criteria are discussed here: *Average* deformation and *Maximum* deformation. 4000 random load distribution cases are applied and the *Average* is the mean value of the norm of the 4000 deformation led by corresponding load distributions. *Maximum* is obtained by applying the load that leads to the maximum norm of deformation: on frame structure, the load distribution is given by the inner optimization of our formulation, i.e., $\max_{F \text{ satisfying } (2)} \frac{(\hat{K}^{-1}F)^T (\hat{K}^{-1}F)}{F^T F}$;

on the final object, the load distribution is given by the result of [27]. In our experiment, the amount of material use is set to be the 20% of the solid volume of the input object. A better global stiffness property means the less value these two criteria are.

All the experiments were conducted on a PC with a 2.8GHZ Core CPU and 8GB RAM, running Linux OS.

To verify the global stiffness property of our optimized frame structure, we compare it and the initial structure with uniform beam radii. The uniform radii is set to make the control structure have the same volume as our result. In Fig. 3, two certain cases of the hand model is presented where warmer color refers to a larger value of deformation and cooler color refers to a smaller value of deformation. For all the tested models, the map of the *Maximum* deformation is illustrated in Fig. 4. With the statistic data in Table 1, our proposed formulation is proved to be able to optimize the global stiffness of a given initial frame structure.

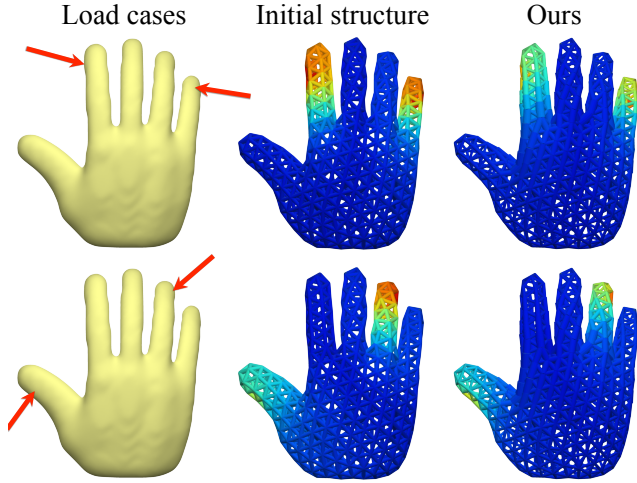


Figure 3: Deformation distribution of two certain load distribution cases (top and bottom row) on the initial structure and our optimized structure of hand model. The red arrows shown on the model indicate that the deformation is simulated under the certain pair of forces. The initial structure we tested have the same volume with our result. Warmer color refers to a larger value of deformation and cooler color refers to a smaller value of deformation. It is obvious that our result performs better in these two selected cases.

Table 1: Statistics of tests for frame structure. Mean values of 4000 records of deformation (in mm) for each model are listed. The maximum deformation value for each model is also listed. First two rows are the results of uniform frame and the last two rows are our results .

Models		American football	Hand	Cactus	Trophy	Molar
Initial structure	Avg.	0.198	0.677	0.781	0.110	0.141
	Max	0.273	1.083	1.264	0.269	0.233
Ours	Avg.	0.193	0.523	0.516	0.106	0.101
	Max	0.256	0.790	0.832	0.258	0.154

Physical experiment simulation For examining the final object generated based on the optimized frame structure, FEM-based computation framework need to be adapted. For an elastic body Ω , the stationary state of objects under forces can be described by the linear elasticity problem,

$$\begin{aligned} -\operatorname{div}(\sigma(\epsilon(u))) &= f, \quad \text{in } \Omega \\ u &= 0, \quad \text{on } \Gamma_D \\ \sigma(\epsilon(u)) \cdot n &= g, \quad \text{on } \Gamma_N. \end{aligned} \tag{11}$$

In this problem, u is displacement, $\epsilon(u) = 1/2(\nabla u + \nabla u^T)$ is the strain, and $\sigma(\epsilon) = 2\mu\epsilon + \gamma(\operatorname{tr}(\epsilon))I$ is the stress. The quantities γ and μ are the Lame moduli of the material. Such a problem can be solved by using FEMs. In our experiment, the FEM computation is executed by using DOLFIN [10].

We compare our results and uniform hollowing solution. In Fig. 5, we show the comparison of the same cases as shown in Fig. 3 for the hand model. General statistic data is shown in Table 2. We also compare our result with [11]. We generate a global stiffness molar model which has the same volume with the molar example provided by this work as shown in Fig. 6. The simulated results show that ours are more suitable under unknown load cases.

Our saddle point optimization problem can be solved very efficiently. All examples appear in this paper are optimized within 20mins.

6 Conclusion

In this work, we propose a novel approach for global stiffness struture optimization and present a saddle point algorithm to solve the optimization problem efficiently. When given a certain amount of material for printing an object in 3D, our approach can generate a global stiffness structure with minimum deformation under all possible force distributions. Our approach also provides a solution for formulating adaptive hollowing and interior supportive structures in a unified form, while optimizing them simultaneously. A number of experimental results have shown the validity and the rationality of our solution, and have proved our proposed approach to be much more applicable than previous methods.

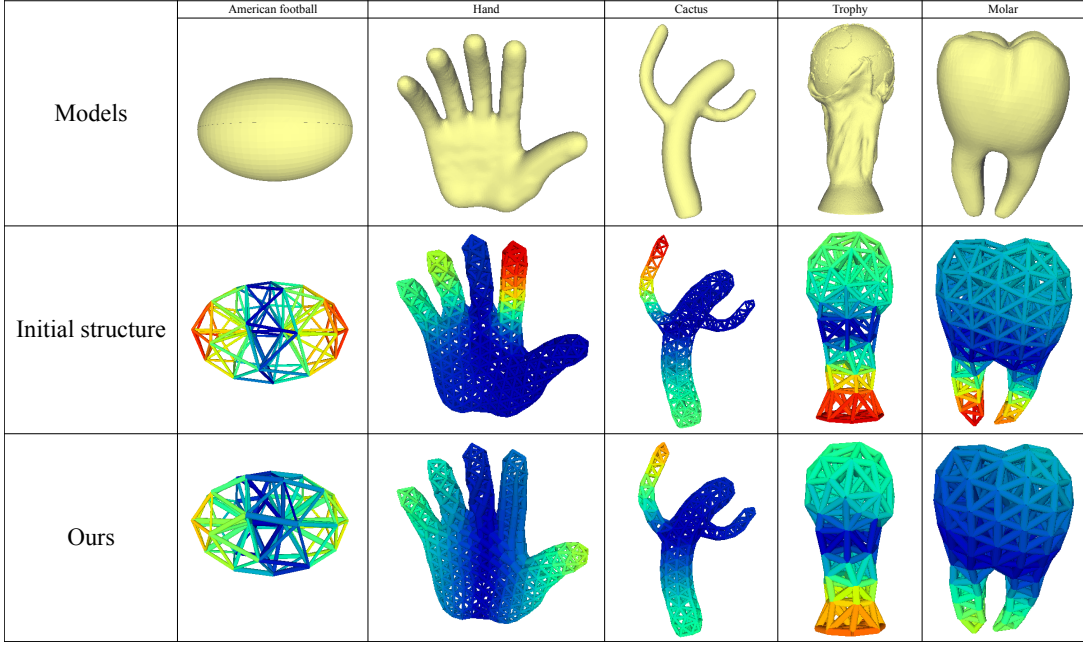


Figure 4: Maximum deformation distribution case for test frame structures. Top: Input model; Middle: distribution map of initial structure; Bottom: distribution map of our optimized structure. The magnitude of maximum deformation on our resulting structure is much smaller than that on the uniform initial frame structure. Note that, for example in the hand model, the worst case is changing during our optimization of the frame structures

Table 2: Statistics of the simulation tests for object. Mean values of 4000 records of deformation (in mm) for each model are listed. The maximum deformation value for each model is also listed. First two rows are the results of uniform hollowing solution and the last two rows are our results .

Models		American football	Hand	Cactus	Trophy	Molar
Uniform hollowing	Avg.	0.138	1.135	1.259	0.998	0.287
	Max	0.201	1.529	2.165	1.486	0.469
Ours	Avg.	0.121	0.972	1.029	0.626	0.106
	Max	0.189	1.347	1.768	1.097	0.158

Limitations and future work Our research opens several future studies in the direction of structural optimization.

In this paper, the optimization’s objective is to minimize the possible deformation of objects. However, the maximum stress distribution inside an object is of more interest in some applications, since it tells us where a crack is likely to happen. For such a need, we should introduce new objective functions. A simple idea is to consider the following optimization problem.

$$\min_{(V,r)} \max_f \frac{\int_{\Omega} |\sigma|^2 dx}{\int_{\Omega} f^2 dx}$$

where σ denotes the stress of the body under a force f .

References

- [1] M. Bächer, E. Whiting, B. Bickel, and O. Sorkine-Hornung. Spin-it: optimizing moment of inertia for spinnable objects. *ACM Transactions on Graphics (TOG)*, 33(4):96, 2014.
- [2] M. P. Bendsoe and O. Sigmund. *Topology optimization: theory, methods and applications*. Springer, 2003.
- [3] B. Bickel, M. Bächer, M. A. Otaduy, H. R. Lee, H. Pfister, M. Gross, and W. Matusik. Design and fabrication of materials with desired deformation behavior. *ACM Trans. on Graphics (Proc. SIGGRAPH)*, 29(3), 2010.
- [4] T. R. Chandrupatla, A. D. Belegundu, T. Ramesh, and C. Ray. *Introduction to finite elements in engineering*. Prentice-Hall Englewood Cliffs, NJ, 1991.
- [5] Y. Chen. 3D texture mapping for rapid manufacturing. *Computer-Aided Design and Applications*, 4(6):761–771, 2007.
- [6] A. Cherkaev, E. Cherkaeva, et al. Stable optimal design for uncertain loading conditions, 1998.
- [7] E. Cherkaev and A. Cherkaev. Principal compliance and robust optimal design. In *The Rational Spirit in Modern Continuum Mechanics*, pages 169–196. Springer, 2004.
- [8] L. J. Gibson and M. F. Ashby. *Cellular Solids: Structure and Properties*. Cambridge University Press, 2nd edition, 1999.
- [9] T. J. R. Hughes. *The Finite Element Method: Linear Static and Dynamic Finite Element Analysis*. Prentice-Hall, 1987.
- [10] A. Logg, G. N. Wells, and J. Hake. *DOLFIN: a C++/Python Finite Element Library*. Springer, 2012.
- [11] L. Lu, A. Sharf, H. Zhao, Y. Wei, Q. Fan, X. Chen, Y. Savoye, C. Tu, D. Cohen-Or, and B. Chen. Build-to-last: Strength to weight 3d printed objects. *ACM Trans. Graph. (Proc. SIGGRAPH)*, 33(4):97:1–97:10, August 2014.
- [12] L. Luo, I. Baran, S. Rusinkiewicz, and W. Matusik. Chopper: partitioning models into 3d-printable parts. *ACM Trans. Graph.*, 31(6):129, 2012.

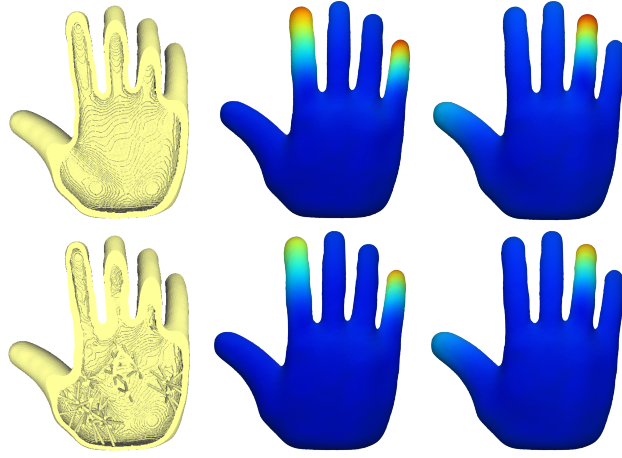


Figure 5: Deformation distribution of the two load distribution cases (same as the cases shown in Fig. 3) on the uniform hollowing result (top) and our optimal result (bottom) of hand model. The first column is the sectional view. The load is acted as pinching the forefinger and the little finger for the second column and pinching the thumb and the third finger for the last column. Two objects we tested have the same volume. It can be observe that the final object generated by our proposed postprocessing can sucessfully inherit the mechanical property and preforms better.

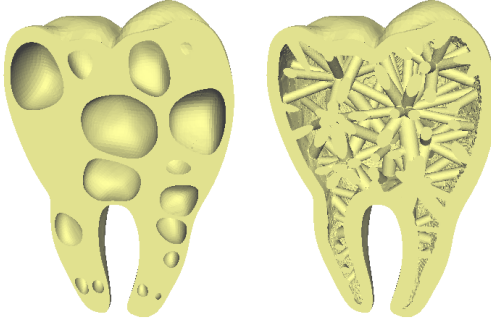


Figure 6: We compare our result with [11]. The left one is provided by [11] and the right one is ours. Two result objects have the same volume and the (Avg., Max) deformation is (0.125,0.197) and (0.106,0.158), respectively.

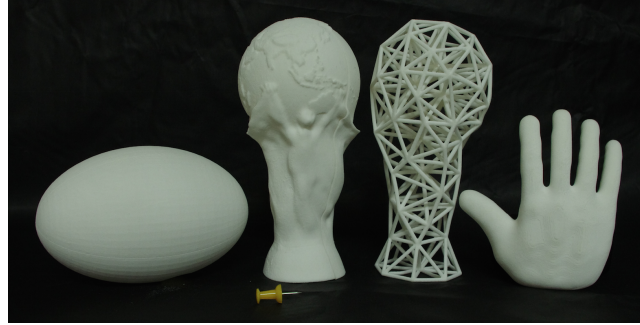


Figure 7: We fabricate the final results for some models.

- [13] J. Nocedal and S. Wright. *Numerical Optimization*. Springer, 2nd edition, 2006.
- [14] B. N. Parlett. *The Symmetric Eigenvalue Problem*. Prentice-Hall, Inc., 1998.
- [15] R. Prevost, E. Whiting, S. Lefebvre, and O. Sorkine-Hornung. Make it stand: balancing shapes for 3D fabrication. *ACM Transactions on Graphics (TOG)*, 32(4):81, 2013.
- [16] G. I. Rozvany. *Structural design via optimality criteria*. Springer, 1989.
- [17] G. I. Rozvany. A critical review of established methods of structural topology optimization. *Structural and Multidisciplinary Optimization*, 37(3):217–237, 2009.
- [18] J. Smith, J. Hodgins, I. Oppenheim, and A. Witkin. Creating models of truss structures with optimization. *ACM Trans. Graph. (Proc. SIGGRAPH)*, 21(3):295–301, 2002.
- [19] O. Stava, J. Vanek, B. Benes, N. Carr, and R. M  ch. Stress relief: improving structural strength of 3D printable objects. *ACM Transactions on Graphics (TOG)*, 31(4):48, 2012.
- [20] A. Takezawa, S. Nii, M. Kitamura, and N. Kogiso. Topology optimization for worst load conditions based on the eigenvalue analysis of an aggregated linear system. *Computer Methods in Applied Mechanics and Engineering*, 200(25):2268–2281, 2011.

- [21] N. Umetani and R. Schmidt. Cross-sectional structural analysis for 3d printing optimization. In *SIGGRAPH Asia 2013 Technical Briefs*, page 5. ACM, 2013.
- [22] C. C. Wang and Y. Chen. Thickening freeform surfaces for solid fabrication. *Rapid Prototyping Journal*, 19(6):395–406, 2013.
- [23] H. Wang, Y. Chen, and D. W. Rosen. A hybrid geometric modeling method for large scale conformal cellular structures. In *ASME 2005 International Design Engineering Technical Conferences and Computers and Information in Engineering Conference*, pages 421–427. American Society of Mechanical Engineers, 2005.
- [24] W. Wang, T. Y. Wang, Z. Yang, L. Liu, X. Tong, W. Tong, J. Deng, F. Chen, and X. Liu. Cost-effective printing of 3d objects with skin-frame structures. *ACM Transactions on Graphics (TOG)*, 32(6):177, 2013.
- [25] D.-M. Yan, B. Lévy, Y. Liu, F. Sun, and W. Wang. Isotropic remeshing with fast and exact computation of restricted voronoi diagram. In *Computer Graphics Forum*, pages 1445–1454. Wiley Online Library, 2009.
- [26] D.-M. Yan, W. Wang, B. Lèvy, and Y. Liu. Efficient computation of 3D clipped Voronoi diagram. In *6th International Conference on Geometric Modeling and Processing (GMP 2010)*, pages 269–282, 2010.
- [27] Q. Zhou, J. Panetta, and D. Zorin. Worst-case structural analysis. *ACM Transactions on Graphics (TOG)*, 32(4):137, 2013.